Thermogravimetric Analysis of the Oxidation of Multiwalled Carbon Nanotubes: Evidence for the Role of Defect Sites in Carbon Nanotube Chemistry

ARTICLE *in* NANO LETTERS · MAY 2002

Impact Factor: 13.59 · DOI: 10.1021/nl020297u

7 AUTHORS, INCLUDING:

David Jacques
university buckingham
24 PUBLICATIONS **2,370** CITATIONS
SEE PROFILE

John P. Selegue
University of Kentucky
122 PUBLICATIONS **3,329** CITATIONS
SEE PROFILE

NANO LETTERS

2002
Vol. 2, No. 6
615−619

Thermogravimetric Analysis of the Oxidation of Multiwalled Carbon Nanotubes: Evidence for the Role of Defect Sites in Carbon Nanotube Chemistry

David Bom,[†] Rodney Andrews,[‡] David Jacques,[‡] John Anthony,[†] Bailin Chen,[†] Mark S. Meier,[†] and John P. Selegue*,[†]

Department of Chemistry, University of Kentucky, Lexington, Kentucky 40506-0055, and Center for Applied Energy Research, University of Kentucky, Lexington, Kentucky 40511-8410

Received February 25, 2002; Revised Manuscript Received April 16, 2002

ABSTRACT

Thermogravimetric analysis (TGA) has demonstrated that multiwalled nanotubes (MWNTs) annealed at 2200 to 2800 °C are more air stable than as-produced MWNTs, diamond, graphite, and annealed diamond. The annealed MWNTs are similar in stability to annealed graphite. Defect sites along the walls and at the ends of the raw MWNTs facilitate the thermal oxidative destruction of the nanotubes. Thermal annealing removes these defects, thereby providing MWNTs with enhanced air stability.

Since their discovery by Iijima, multiwalled nanotubes (MWNTs)[1] and single-walled nanotubes (SWNTs)[2,3] continue to draw attention from the scientific community for their myriad potential applications. A few of these applications include new high-strength composites,[4] electronic components,[5,6] and the storage of a variety of gases,[7] of which hydrogen has been of particular interest.[8−12]

SWNTs and MWNTs are cylindrical allotropes of carbon. Single-wall nanotubes consist of a single cylinder of graphite, while MWNTs contain multiple graphite cylinders nesting within each other. There are three predominant methods for the synthesis of SWNTs and MWNTs: electric arc discharge, laser ablation of a carbon target, and chemical vapor deposition (CVD).[13,14]

The CVD method involves simultaneous decomposition of a carbon source with a metal catalyst in a heated tube furnace under an atmosphere of H_2 and Ar. One approach to the CVD generation of MWNTs uses xylenes as a carbon source and ferrocene as catalyst.[15] A second approach, referred to as the HiPCO process, uses CO and $Fe(CO)_5$ to produce SWNTs.[16] It is thought that the mechanism of MWNT and SWNT growth involves decomposition of the carbon feedstock, followed by dissolution of the carbon phase into a metal nanoparticle and redeposition of carbon on the catalyst surface as a growing nanotube.[13,14] Metal catalyst particle size has been correlated with nanotube diameter.[17] These processes introduce structural defects as the nanotubes form. Evidence for the defective nature of these materials is seen in numerous published SEM and TEM images.[15,18]

Defect sites in graphite and diamond contribute to a decrease in the oxidative stability of these materials. Defects in graphite[19] and diamond[20] include edges, dangling bonds, vacancies, dislocations, and steps. These defect sites are particularly reactive to oxygen at elevated temperatures. Basal planes and ⟨111⟩ planes (diamond) are the least reactive toward oxidation.[19,21] In addition to edges and dangling bonds, nanotubes also contain 5,7-ring defects in which a five-membered and seven-membered ring are fused together to form an azulene unit, which substitutes for a naphthalene unit in the graphene network.[13,14] Defects, including five-membered rings, are responsible for closing the ends of nanotubes. Defects are also present at bends, Y-junctions, and kinks in nanotubes. Using the V-ridge technology, Lu et al. introduced kinks into nanotubes and demonstrated, using scanning electron microscopy, that high-temperature air oxidation occurred preferably at these kink sites.[22] Ozonolysis has been used to quantitate the defect density in SWNTs.[23] In addition to defects, the oxidative stability of carbon nanotubes is also influenced by nanotube diameter.[24]

* Corresponding author: selegue@uky.edu; 859-257-3484; 859-323-1069 (Fax).
[†] Department of Chemistry.
[‡] Center for Applied Energy Research.

10.1021/nl020297u CCC: $22.00
Published on Web 05/03/2002

A smaller diameter results in a higher degree of curvature and subsequently a higher reactivity toward oxygen. High curvature is also responsible for the poor air stability of C_{60} and C_{70} at elevated temperatures.[25,26]

Thermogravimetric analysis (TGA) has been used to study the oxidative stability of graphite, diamond, C_{60}, C_{70}, and nanotubes (SWNTs and MWNTs).[18,21,25−34] TGA has also been used to investigate the adsorption of gases on the inner and outer walls of carbon nanotubes.[7,35,36] This paper describes a TGA investigation of the impact of thermal annealing on the oxidative stability of CVD-grown MWNTs, including comparisons to common carbon phases such as graphite and diamond.

A wide variety of analytical techniques, including high-resolution transmission electron microscopy (HRTEM), scanning electron microscopy (SEM), atomic force microscopy (AFM),[37−39] ESR,[40] and Raman spectroscopy have been used to study nanotubes.[13,14,22,41,42] Recently, HRTEM was used to study the effects of thermal annealing on the defect density of CVD-grown MWNTs.[43] As the annealing temperature was raised, the interlayer distance between nanotube walls decreased, suggesting higher order and diminishing defect density. Atomic force microscopy demonstrated that raw (more defective) nanotubes are more elastic than thermally annealed nanotubes.[44] Raw and annealed nanotubes were also studied using ESR.[40] Comparison of the *g* values before and after annealing showed a strong temperature dependence for the raw material, while the *g* value for the annealed nanotubes remained constant over a temperature range of 4 to 300 K. The behavior of the annealed nanotubes was very similar to graphite, suggesting that the annealing process had removed defects from the walls of the nanotubes. HRTEM, SEM, and AFM provide useful data about the intimate structure of selected nanotubes in a sample, but very little information about the sample as a whole. While Raman and ESR spectroscopy analyze the bulk sample, they do not provide information about the overall stability gained through graphitization. Although CVD methods can produce large amounts of material, new methods are needed for quality control.[15] Ideal methods should focus on analysis of nanotube samples as a whole rather than analysis of single nanotubes. The work presented herein provides a rapid, inexpensive method for the batch stability analysis of raw and graphitized nanotubes.

Raw MWNTs were prepared in a tube furnace by CVD using xylenes and ferrocene at 650, 700, 750, or 800 °C.[15] The raw nanotubes synthesized at 800 °C were annealed at 1600, 2250, and 2800 °C in a horizontal, electric-resistance tube furnace.[43] Natural diamond powder (48,357-5, 1−2 micron) and graphite (28,286-3, 1−2 micron) were obtained from Aldrich and subjected to the same conditions as outlined above for MWNTs. Samples of diamond and graphite were graphitized at 2800 °C, resulting in a 4.00% mass loss for graphite and a 0.08% mass increase for diamond. The multiwalled nanotubes annealed at 1600, 2200, and 2800 °C underwent mass losses of 2.90%, 5.80% and 7.50%, respectively. The 7.50% mass loss corresponds to the expected iron content in the raw MWNTs.[43]

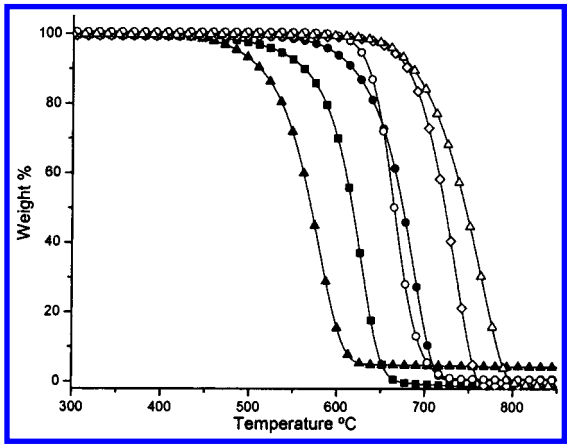

Figure 1. Weight loss curves for raw MWNTs, diamond, annealed diamond, graphite, annealed MWNTs and annealed graphite: ▲ raw MWNTs; ■ diamond; ○ annealed diamond; ● graphite; ◇ annealed MWNTs; △ annealed graphite.

Thermogravimetric analyses were performed on a TA Instruments Hi Res TGA 2950 thermogravimetric analyzer equipped with an EGA furnace. Samples were analyzed in platinum pans at a heating rate of 1 °C/min to 1000 °C in an atmosphere of air flowing at 180 mL/min. Sample masses ranged from 5−12 mg. Sample purification was not required, because the purity of the raw MWNTs is 92.5% to 97.1%. The only impurities present in the raw nanotubes were a thin layer of amorphous carbon on the nanotube surface and the encapsulated iron catalyst residue. There were not any amorphous carbon nanoparticles. Purity was assessed by SEM and HRTEM analyses.[15,43]

Thermogravimetric analysis was used to study the effect of annealing on the oxidative stability of MWNTs, diamond, and graphite (Figure 1). Prior to graphitization, the raw nanotubes were considerably less stable to high-temperature oxidation than graphite and diamond powder. In each case, thermal annealing at 2800 °C produced material that was more thermally stable toward air than the unannealed material. The oxidative stability enhancements of annealed graphite, diamond, and MWNTs were 51, 70, and 155 °C. After annealing, the MWNTs are *more* stable toward thermal oxidative destruction than annealed diamond and similar in stability to annealed graphite. Annealed MWNTs are significantly more stable than unannealed diamond and graphite.

TEM analysis of raw MWNTs suggests that these materials contain numerous defects along the walls and at the ends of the tubes.[15,43] These defects likely lead to oxidative instability by providing edges and dangling bonds by which each nanotube layer can be "unzipped" and peeled away, resulting in combustion at a lower temperature than graphite or diamond. As each layer is removed, new defect sites are exposed and the process continues.

High-temperature graphitization anneals out many defects, reducing the defect density and producing more perfect MWNTs, diamond, and graphite. With fewer defects, these materials display greater stability toward high-temperature oxidation than raw MWNTs, graphite, and diamond. Comparison of the remarkable stability enhancement for annealed MWNTs with the modest enhancements for graphite and

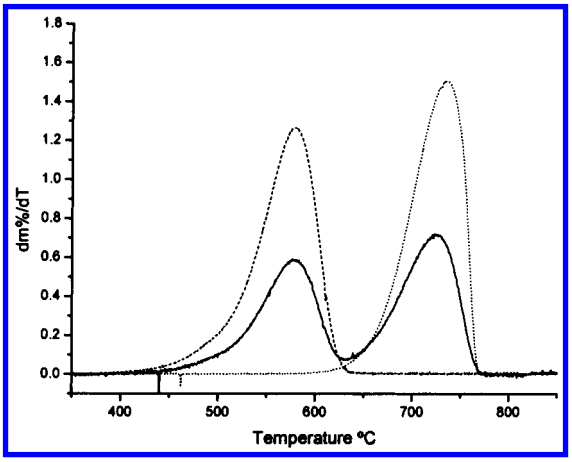

Figure 2. First derivative plots of the thermogravimetric analysis of mixed raw and graphitized MWNTs vs unmixed controls: -- unmixed raw MWNTs; — mixed raw and graphitized MWNTs; ••• unmixed graphitized MWNTs.

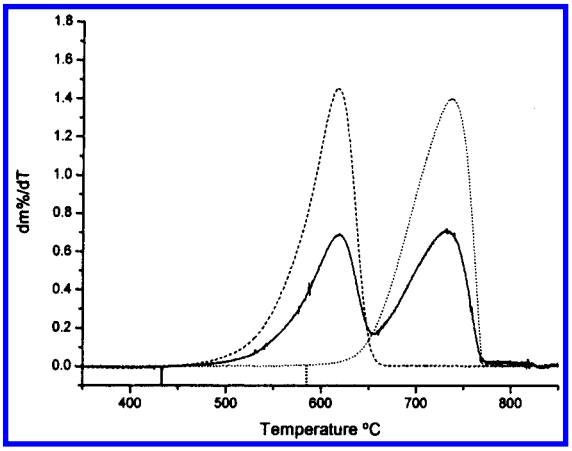

Figure 3. First derivative plots of the thermogravimetric analysis of mixed graphitized MWNTs (1600 °C and 2200 °C) vs unmixed controls: -- MWNTs graphitized at 1600 °C; — mixed graphitized MWNTs; ••• MWNTs graphitized at 2200 °C.

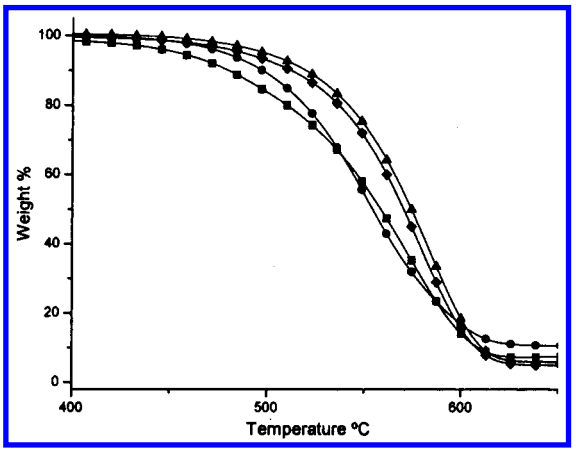

Figure 4. Thermogravimetric analysis of raw MWNTs synthesized at 650 °C, 700 °C, 750 °C, and 800 °C: ● MWNTs prepared at 650 °C; ■ MWNTs prepared at 700 °C; ▲ MWNTs prepared at 750 °C; ◆ MWNTs prepared at 800 °C.

diamond suggests that raw MWNTs contain more defects than unannealed samples of diamond and graphite. The annealing process removes most of the defect sites from the MWNTs, resulting in a thermal oxidative stability similar to annealed graphite.

Since the arc preparation of MWNTs occurs under extremely high-energy conditions, as-obtained arc MWNTs are highly graphitic and probably closely resemble our graphitized nanotubes. Indeed, a comparison of the TGA results reported by Pang et al. with our own data supports this idea.[27] However, our graphitized MWNTs undergo combustion at a slightly higher temperature than the raw arc-grown material. This phenomenon could be due to the absence of nanoparticles in our graphitized samples. Nanoparticles, which comprise 75% of the Pang material, could account for their lower combustion temperature. Murphy et al. recently published the TGA analysis of arc-grown MWNT soot. Taking into account Murphy's more rapid TGA heating rate (10 °C/min by Murphy vs 1 °C/min by Pang), their results are similar to Pang's.[34] Since annealing at 2800 °C removes essentially all of the iron catalyst residue from CVD MWNTs, it is not certain whether a reduction in defect sites, or simply a reduction in iron content is fully responsible for the dramatic increase in stability.[43]

To test whether graphitized MWNTs are less oxidatively stable in the presence of extrinsic iron, we analyzed an equal-mass mixture of raw and graphitized (2800 °C) MWNTs by TGA. Figure 2 clearly shows independent oxidation of each component, with a minimum combustion rate centered around 633 °C. We conclude that combustion of the graphitized tubes was unaffected by the presence of catalyst particles from the raw MWNTs. The onset temperature of combustion and the T_{max} (temperature at which the rate of combustion is highest) for the raw and graphitized components of the mixture compare well with each of the unmixed controls, although the rates of combustion were slightly slower than the unmixed controls. A one-to-one ratio of nanotubes graphitized at 1600 °C and 2200 °C oxidized similarly (Figure 3).

Lee et al. reported that higher synthesis temperatures resulted in more highly crystalline nanotubes.[33] Their TGA plots showed significant increases in nanotube oxidative stability as the synthesis temperature was increased from 750 to 950 °C. Based on a combination of Lee's observations and our own, we conjectured that nanotubes prepared at a higher temperature would exhibit greater oxidative stability because defects would be annealed out as the nanotubes are formed. Accordingly, we used TGA to analyze MWNTs prepared at 650, 700, 750, and 800 °C (Figure 4). In contrast to Lee's results, a strong correlation of synthesis temperature with the onset of nanotube combustion was *not* observed. Probably 800 °C is not a high enough temperature for significant annealing to take place. Increasing synthesis temperature did lead to decreasing residual iron catalyst, as shown by the decreasing mass of residue in the TGA analyses. Visual inspection of the red TGA residue suggests that it is Fe_2O_3. Unfortunately, powder X-ray diffraction did not confirm the identity of the residue because it is amorphous.

The decreasing iron concentration is the result of increased carbon yields at the higher synthesis temperatures, providing

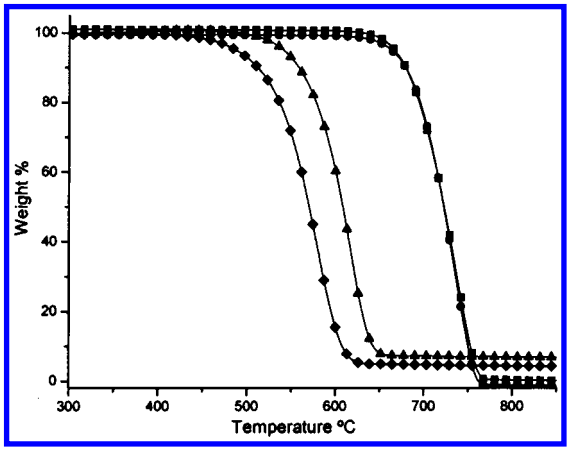

Figure 5. Thermogravimetric analysis of MWNTs graphitized at 1600 °C, 2200 °C, and 2800 °C relative to raw MWNTs: ◆ raw MWNTs; ▲ MWNTs graphitized at 1600 °C; ■ MWNTs graphitized at 2200 °C; ● MWNTs graphitized at 2800 °C.

a dilution of the iron catalyst within the sample. Furthermore, if decreasing iron content were responsible for increasing tube stability, then we would expect markedly improved stability for those raw samples that contain lower concentrations of iron catalyst residue. Since all four samples underwent combustion at essentially the same temperature, we concluded that residual iron catalyst has little or no effect on nanotube oxidative stability. Since the iron catalyst particles are encapsulated within the nanotubes and because oxidation presumably occurs at the surface of the nanotubes, the catalyst particles should not be involved until late in combustion. We do *not* observe an abrupt acceleration in combustion during our analysis.

Next, we investigated the influence of the graphitization temperature on MWNT oxidative stability. We analyzed samples of graphitized MWNTs annealed at 1600, 2200, and 2800 °C (Figure 5). The sample graphitized at 1600 °C underwent combustion at a higher temperature than the raw material, but considerably lower than the samples annealed at 2200 °C and 2800 °C. Furthermore, since 1600 °C is below the boiling point of iron, this sample contained residual catalyst.[43] The samples annealed at 2200 and 2800 °C, containing little or no catalyst residue, underwent combustion at very similar temperatures.

Graphitization at 1600 °C resulted in the removal of some, but not all, defects, providing MWNTs that were more stable than the raw MWNTs. Treatment at 2200 and 2800 °C annealed out even more of the defect sites, thereby significantly improving nanotube oxidative stability relative to both the raw MWNTs and the MWNTs annealed at 1600 °C. These ideas are further supported by previous work in which increasing graphitization temperature correlated with decreasing interlayer spacing.[43] Interestingly, the interlayer spacing of the MWNTs treated at 2800 °C was considerably smaller than the spacing of the tubes graphitized at 2200 °C, yet the oxidative stability of nanotubes annealed at 2800 °C is not improved over those annealed at 2200 °C. This observation suggests that most defects are annealed out at 2200 °C. Furthermore, since the difference between the combustion temperatures of MWNTs annealed at 2200 and 2800 °C was so small, it seems that higher temperatures do not further enhance stability. Nanotubes graphitized at 2200 and 2800 °C still undergo oxidative degradation, suggesting that the few remaining defects, dangling bonds, or edges are limited to the ends of the tubes where high curvature is present. In fact, independent work by Tsang et al. and Ajayan et al. demonstrated that thinning and opening of arc-grown MWNTs are limited to the ends of the nanotubes when they are treated with CO_2 at 850 °C or air at 800 °C.[45,46]

We have analyzed the thermal oxidative stability of raw MWNTs, prepared by CVD using xylenes as the carbon source and ferrocene as catalyst, with and without graphitization at 1600, 2200, and 2800 °C. We compared the stabilities of these MWNTs to annealed and unannealed samples of graphite and diamond.

The raw, ungraphitized MWNTs underwent oxidation at a significantly lower temperature than graphite or diamond. We believe that this lower relative stability is due to the presence of numerous defects along the walls and at the ends of the nanotubes. Similar to observations made by other researchers, these defects enhance the combustion of the nanotubes. Annealed MWNTs are nearly as oxidatively stable as annealed graphite. The stability enhancements achieved by annealing MWNTs was significantly higher than the stability enhancements of annealed diamond and graphite, suggesting that raw MWNTs are more defective than diamond and graphite. Graphitization of the raw material at 2200 and 2800 °C produces MWNTs of increased thermal oxidative stability, compared to material graphitized at 1600 °C. MWNTs graphitized at 2200 and 2800 °C display similar oxidative stabilities to each other and annealed graphite, but better oxidative stability than unannealed graphite, diamond, or annealed diamond. Higher synthesis temperatures did not improve the stability of the raw material but did result in diminishing levels of residual iron catalyst.

Previous nanotube analyses have relied on high-resolution transmission electron microscopy (HRTEM) to provide information about the graphitization of MWNTs. Although HRTEM provides a useful visual method to analyze MWNTs, it provides information limited to only a few nanotubes, rather than the nanotube sample as a whole. The TGA method described here provides an inexpensive, straightforward, fast means of characterizing the stability of a nanotube sample toward high-temperature air oxidation and of assaying the impact of graphitization. The large-scale synthesis of CVD-grown nanotubes has been realized, but few methods exist for the convenient quality control of bulk samples of nanotubes. We have demonstrated that thermogravimetric analysis is useful in filling this void.

Acknowledgment. We thank the National Science Foundation (Materials Research Science and Engineering Center award DMR-9809686) and the U.S. Department of Energy (DE-FG02-00ER45847), the Center for Applied Energy Research (CAER), and the Department of Chemistry at the University of Kentucky for financial support of this work.

References

(1) Iijima, S. *Nature (London)* **1991**, *354*, 56−58.
(2) Iijima, S.; Ichihashi, T. *Nature (London)* **1993**, *363*, 603−605.
(3) Bethune, D. S.; Kiang, C. H.; de Vries, M. S.; Gorman, G.; Savoy, R.; Vazquez, J.; Beyers, R. *Nature (London)* **1993**, *363*, 605−607.
(4) Lahr, B.; Sandler, J. *Kunststoffe* **2000**, *90*, 94−96.
(5) White, C. T.; Todorov, T. N. *Nature (London)* **2001**, *411*, 649−651.
(6) Colbert, D. T.; Smalley, R. E. *Trends Biotechnol.* **1999**, *17*, 46−50.
(7) Long, R. Q.; Yang, R. T. *Ind. Eng. Chem. Res.* **2001**, *40*, 4288−4291.
(8) Darkrim, F. L.; Malbrunot, P.; Tartaglia, G. P. *Int. J. Hydrogen Energy* **2001**, *27*, 193−202.
(9) Darkrim, F.; Aoufi, A.; Levesque, D. *Mol. Simul.* **2000**, *24*, 51−61.
(10) Maniwa, Y.; Kumazawa, Y.; Saito, Y.; Tou, H.; Kataura, H.; Ishii, H.; Suzuki, S.; Achiba, Y.; Fujiwara, A.; Suematsu, H. *Mol. Cryst. Liq. Cryst. Sci. Technol., Sect. A* **2000**, *340*, 671−676.
(11) Sumanasekera, G. U.; Adu, C. K. W.; Pradhan, B. K.; Chen, G.; Romero, H. E.; Eklund, P. C. *Phys. Rev. B: Cond. Matter Mater. Phys.* **2002**, *65*, 035408/1−035408/5.
(12) Hirscher, M.; Becher, M.; Haluska, M.; Dettlaff-Weglikowska, U.; Quintel, A.; Duesberg, G. S.; Choi, Y. M.; Downes, P.; Hulman, M.; Roth, S.; Stepanek, I.; Bernier, P. *Appl. Phys. A: Mater. Sci. Process.* **2001**, *72*, 129−132.
(13) Sinnott, S. B.; Andrews, R. *Crit. Rev. Solid State Mater. Sci.* **2001**, *26*, 145−249.
(14) Harris, P. J. F. *Carbon Nanotubes and Related Structures: New Materials for the Twenty-first Century.*; Press Syndicate of the University of Cambridge: Cambridge, 2001.
(15) Andrews, R.; Jacques, D.; Rao, A. M.; Derbyshire, F.; Qian, D.; Fan, X.; Dickey, E. C.; Chen, J. *Chem. Phys. Lett.* **1999**, *303*, 467−474.
(16) Bronikowski, M. J.; Willis, P. A.; Colbert, D. T.; Smith, K. A.; Smalley, R. E. *J. Vac. Sci. Technol. A* **2001**, *19*, 1800−1805.
(17) Sinnott, S. B.; Andrews, R.; Qian, D.; Rao, A. M.; Mao, Z.; Dickey, E. C.; Derbyshire, F. *Chem. Phys. Lett.* **1999**, *315*, 25−30.
(18) Chiang, I. W.; Brinson, B. E.; Huang, A. Y.; Willis, P. A.; Bronikowski, M. J.; Margrave, J. L.; Smalley, R. E.; Hauge, R. H. *J. Phys. Chem. B* **2001**, *105*, 8297−8301.
(19) Walker, P. L., Jr. *Carbon* **1990**, *28*, 261−279.
(20) McKee, D. W. *Chem. Phys. Carbon* **1981**, *16*, 1−118.
(21) Joshi, A.; Nimmagadda, R.; Herrington, J. *J. Vac. Sci. Technol. A* **1990**, *8*, 2137−2142.
(22) Lu, X.; Ausman, K. D.; Piner, R. D.; Ruoff, R. S. *J. Appl. Phys.* **1999**, *86*, 186−189.
(23) Mawhinney, D. B.; Naumenko, V.; Kuznetsova, A.; Yates, J. T.; Liu, J.; Smalley, R. E. *Chem. Phys. Lett.* **2000**, *324*, 213-216.
(24) Yao, N.; Lordi, V.; Ma, S. X. C.; Dujardin, E.; Krishnan, A.; Treacy, M. M. J.; Ebbesen, T. W. *J. Mater. Res.* **1998**, *13*, 2432−2437.
(25) Saxby, J. D.; Chatfield, S. P.; Palmisano, A. J.; Vassallo, A. M.; Wilson, M. A.; Pang, L. S. K. *J. Phys. Chem.* **1992**, *96*, 17−18.
(26) Gallagher, P. K.; Zhong, Z. *J. Therm. Anal.* **1992**, *38*, 2247−2255.
(27) Pang, L. S. K.; Saxby, J. D.; Chatfield, S. P. *J. Phys. Chem.* **1993**, *97*, 6941−6942.
(28) Crumpton, D. M.; Laitinen, R. A.; Smieja, J.; Cleary, D. A. *J. Chem. Educ.* **1996**, *73*, 590−591.
(29) Coleman, J. N.; O'Brien, D. F.; Panhuis, M.; Dalton, A. B.; McCarthy, B.; Barklie, R. C.; Blau, W. J. *Synth. Met.* **2001**, *121*, 1229−1230.
(30) Liu, S.; Tang, X.; Mastai, Y.; Felner, I.; Gedanken, A. *J. Mater. Chem.* **2000**, *10*, 2502−2506.
(31) Zhang, H.; Wang, D.; Xue, X.; Chen, B.; Peng, S. *J. Phys. D: Appl. Phys.* **1997**, *30*, L1-L4.
(32) Shi, Z.; Lian, Y.; Liao, F.; Zhou, X.; Gu, Z.; Zhang, Y.; Iijima, S. *Solid State Commun.* **1999**, *112*, 35−37.
(33) Lee, C. J.; Park, J.; Huh, Y.; Lee, J. Y. *Chem. Phys. Lett.* **2001**, *343*, 33−38.
(34) Murphy, R.; Coleman, J. N.; Cadek, M.; McCarthy, B.; Bent, M.; Drury, A.; Barklie, R. C.; Blau, W. J. *J. Phys. Chem. B* **2002**, *106*, 3087−3091.
(35) Pinkerton, F. E.; Wicke, B. G.; Olk, C. H.; Tibbetts, G. G.; Meisner, G. P.; Meyer, M. S.; Herbst, J. F. *J. Phys. Chem. B* **2000**, *104*, 9460−9467.
(36) Wu, X. B.; Chen, P.; Lin, J.; Tan, K. L. *Int. J. Hydrogen Energy* **1999**, *25*, 261−265.
(37) Zhao, B.; Hu, H.; Niyogi, S.; Itkis, M. E.; Hamon, M. A.; Bhowmik, P.; Meier, M. S.; Haddon, R. C. *J. Am. Chem. Soc.* **2001**, *123*, 11673−11677.
(38) Maiti, A. *Chem. Phys. Lett.* **2000**, *331*, 21−25.
(39) Falvo, M. R.; Clary, G. J.; Taylor, R. M., II.; Chi, V.; Brooks, F. P., Jr.; Washburn, S.; Superfine, R. *Nature (London)* **1997**, *389*, 581−584.
(40) Kosaka, M.; Ebbesen, T. W.; Hiura, H.; Tanigaki, K. *Chem. Phys. Lett.* **1995**, *233*, 47−51.
(41) Fink, J. H.; Lambin, P. *Top. Appl. Phys.* **2001**, *80*, 247−272.
(42) Kuzmany, H.; Hulman, M.; Plank, W. *NATO Sci. Ser., II* **2000**, *6*, 243−258.
(43) Andrews, R.; Jacques, D.; Qian, D.; Dickey, E. C. *Carbon* **2001**, *39*, 1681−1687.
(44) Salvetat, J.-P.; Kulik, A. J.; Bonard, J.-M.; Briggs, G. A. D.; Stoeckli, T.; Metenier, K.; Bonnamy, S.; Beguin, F.; Burnham, N. A.; Forro, L. *Adv. Mater. (Weinheim, Ger.)* **1999**, *11*, 161−165.
(45) Tsang, S. C.; Harris, P. J. F.; Green, M. L. H. *Nature (London)* **1993**, *362*, 520−522.
(46) Ajayan, P. M.; Ebbesen, T. W.; Ichihashi, T.; Iijima, S.; Tanigaki, K.; Hiura, H. *Nature (London)* **1993**, *362*, 522−525.

NL020297U